Model of *K*-edge absorption in a hot, dense plasma

J. Al-Kuzee,[1] T. A. Hall,[1] and H-D. Frey[2]
[1]*Department of Physics, University of Essex, Colchester CO4 3SQ, United Kingdom*
[2]*Max-Planck-Institut für Quantenoptik, D-85748 Garching, Germany*
(Received 6 November 1997; revised manuscript received 2 February 1998)

A theoretical model for the calculation of the shape and position of the *K*-shell absorption edge in a hot, dense plasma is described. In the model, degeneracy and continuum lowering contributions due to free electrons are treated as perturbations on the continuum and the bound state. The effect of fluctuations is taken into account by the use of the first neighbor distribution function which is used to form the weighted average of the spectrum due to the first shell of ions surrounding the central ion. The model is used to predict the shape of the aluminum *K*-absorption edge over a range of compression ratios from 1 to 8 and temperatures from 1 to 25 eV. It is found that, at modest temperatures and densities, the shift is compression dependent rather than temperature dependent, whereas the width of the *K* edge is temperature dependent rather than compression dependent. Under more extreme conditions both the shift and the width become dependent on both the temperature and the density. The results for the shift from our model are compared with other theoretical models.
[S1063-651X(98)01206-9]

PACS number(s): 52.25.Nr, 52.50.Lp, 31.15.Bs, 32.30.Rj

I. INTRODUCTION

Early experimental results to measure the shift of an absorption edge in a dense plasma were reported by Bradley *et al.* [1]. The structure and position of the *K* edge of chlorine were observed when a layer of KCl was preheated to several eV and compressed by a strong shock to several times solid density.

Godwal and Lee [2] presented a theoretical model for the calculation of the shift of the *K* edge in a dense plasma. In their model, degeneracy and continuum lowering contributions due to free electrons and neighboring ions were treated as perturbations on the continuum and bound states. These contributions were evaluated using first-principles solid state methods. Their model was used to interpret recently observed shifts in the *K*-edge energy in shock-compressed aluminum [3].

In dense plasmas the ions are strongly correlated [4,5] and we need to consider the form of the radial distribution function [6–9] which describes the local structure around a given ion (short-range order). There are three factors which contribute to the shift of the *K* edge. When the outer electrons are ionized, the shielding of the core electrons is reduced and the *K*-shell electron energies are shifted. This factor can be calculated accurately using Hartree-Fock methods [10]. The second factor is due to the degeneracy or partial degeneracy of the free-electron states, and, as a consequence, there is a lower probability of *K* electrons being excited into one of the states above the Fermi energy. This contribution can be expressed analytically. The third factor arises from the reduction of the ionization level by the electric field due to surrounding plasma electrons and ions (plasma shift). This factor is the least well understood, and was dealt with by Stewart and Pyatt [11] using a model based on the Thomas-Fermi (TF) model [12,13]. The TF model is an average atom model, and, because of this, it can not directly predict the effect of the fluctuations within the plasma.

In our model we consider the state of a local ion. The Thomas-Fermi model is used to calculate the ionization of a local ion with a particular interionic spacing. From this, the *K*-shell energies for an isolated ion and the plasma edge shift for that ion are then calculated. This process is repeated for a distribution of ions with different interionic spacings. The distribution of ions is the nearest neighbor distribution derived from the one component plasma (OCP) model. The total absorption edge is then calculated by weighting the *K*-shell energy shift and the plasma edge shift with this distribution of ion spacings. Finally, the free electron density is calculated using the weighted local ion distribution, and the degree of degeneracy and its effect on the absorption edge is incorporated.

II. MODEL

The TF average atom model was developed by More [14], and provides a general framework for calculating properties of matter at high density and temperature. It is well suited to the treatment of heavy atoms having many thermally excited bound electrons. In addition, the self-consistent-field (SCF) method incorporates the main density effects: pressure ionization, short-range ion screening, and the possible degeneracy of free electrons. The atom is represented as a point nucleus located at the center of a spherical cavity of radius a, in a continuous background of a positive charge. The cavity radius is fixed by the material density. The electron distribution is calculated from a self-consistent average potential, and the chemical potential is chosen so that the sphere is electrically neutral. If the exterior positive charge is exactly equal to the exterior electron density, then the potential vanishes for all $r \geqslant a$. This stronger boundary condition is also sometimes called the ion sphere model. The SCF, average atom model assigns a fractional occupation to each one-electron state according to the Fermi-Dirac statistics of noninteracting electrons.

For a plasma with density ($\rho = 3/4\pi a^3$), temperature T,

and average ionization state Z^*, the K-edge energy is defined as

$$E_1(\rho,T)=E_0(Z^*)+\Delta E_1(\rho,T)+\Delta E_{\rm deg}(\rho,T). \quad (1)$$

The first term $E_0(Z^*)$ is the average K-shell ionization energy of an isolated ion with charge Z^*. The continuum lowering contribution, $\Delta E_1(\rho,T)$, represents the change in the energy of the bound-electron state due to screening of the ion core by neighboring free electrons and ions. Finally, the degeneracy term $\Delta E_{\rm deg}(\rho,T)$ represents the energy of a free electron due to partial degeneracy and interactions with other electrons and ions.

The first step toward calculating the K-edge energy requires the determination of the average ionization state Z^* of the plasma at a given density and temperature. Several attempts have been made to calculate the average ionization state Z^*, such as the augmented-plane-wave method [15], and the complete screened Coulomb potential ionization equilibrium equation of state form of the modified Saha ionization theory [16].

In the present work we initially follow the work of Stewart and Pyatt [11], whose basic equation for the potential distribution, in dimensionless form, is

$$\frac{1}{x}\frac{d^2}{dx^2}(xy)=\frac{1}{Z^*+1}\left[\frac{F_{1/2}(y-\eta)}{F_{1/2}(-\eta)}-\exp(-Z^*y)\right], \quad (2)$$

where $y=eV/kT$, e is the electronic charge, V is the electrostatic potential as a function of distance r, $x=r/D$, D is the Debye length including ions and electrons, η is the degeneracy parameter, and $F_{1/2}(-\eta)$ and $F_{1/2}(y-\eta)$ are the complete Fermi-Dirac functions:

$$F_{1/2}(-\eta)=\int_0^\infty \frac{t^{1/2}dt}{e^{t+\eta}+1}, \quad F_{1/2}(y-\eta)=\int_0^\infty \frac{t^{1/2}dt}{e^{t+\eta-y}+1}.$$

Stewart and Pyatt did not treat the ion whose nucleus is Z entirely by the TF model in order to isolate and evaluate the effect of the free electrons and neighboring ions on the potential distribution. Since the density distribution of these perturbers depends somewhat on the bound-electron distribution, they assumed a bound-electron distribution in order to find the free-electron distribution and the neighboring ion distribution. Having done so by means of the TF model, which approximates the average bound-electron distribution, they applied this same perturbing potential to better models for the unperturbed bound-electron states, such as those of the isolated ion.

The perturbing potential ϕ_s also satisfies Poisson's equation, in which only the free-electron and ion densities appear. In dimensionless form this equation is

$$\frac{1}{x}\frac{d^2}{dx^2}(x\phi)=\frac{1}{Z^*+1}\left[\frac{F_{1/2}(y-\eta,y)}{F_{1/2}(-\eta)}-\exp(-Z^*y)\right], \quad (3)$$

where $\phi=e\phi_s/kT$ and $F_{1/2}(y-\eta,y)$ is the incomplete Fermi-Dirac function

$$F_{1/2}(y-\eta,y)=\int_y^\infty \frac{t^{1/2}dt}{e^{t+\eta-y}+1}.$$

The integration of the right hand side of Eq. (3) over x from zero to infinity gives the quantum mechanical expectation value, averaged over the orbital from which the electron is being removed, and the lowering ionization potential $\Delta E_1(\rho,T)$ can be measured by this quantity in units of kT as follows:

$$\Delta E_1(\rho,T)=-\frac{1}{Z^*+1}\int_0^\infty\left[\frac{F_{1/2}(y-\eta,y)}{F_{1/2}(-\eta)}-\exp(-Z^*y)\right]x\,dx. \quad (4)$$

Unlike Stewart and Pyatt, we do not describe the ions $n_i(x)$ by nonrelativistic Maxwell-Boltzmann statistics, but in terms of the radial distribution function $g(x)$, assuming that the ion density is given by $n_i(x)=\rho g(x)$, and the electron density is given by $n_e(x)=Z^*n_i(x)$. Since the density distribution of these perturbers depends on the bound-electron distribution, we must assume a bound-electron distribution in order to find the free-electron distribution. Having done so by means of the TF model, which approximates the average bound-electron distribution, we may apply this same perturbing potential to better models for the unperturbed bound-electron states, such as those of the isolated ion. Then Eq. (4) can be rewritten as

$$\Delta E_1(\rho,T)=-\frac{kT}{Z^*+1}\int_0^\infty\left[\frac{F_{1/2}(y-\eta,y)}{F_{1/2}(-\eta)}-g(x)\right]x\,dx. \quad (5)$$

The authors of Ref. [13] reported another form of TF model which includes the electron density only as follows:

$$\frac{1}{s}\frac{d^2\beta}{ds^2}=F_{1/2}\left(\frac{\beta}{s}\right), \quad (6)$$

where $s=r/c$, $c=[h^3/(32\pi^2e^2m(2mkT)^{1/2})]^{1/2}$, $\beta/s=(eV/kT)-\eta$, and $F_{1/2}(\beta/s)$ is the complete Fermi-Dirac function. Using this transformation, Eq. (5) can be written in a more convenient form by making the substitutions

$$x=\frac{cs}{D},$$

$$y=\frac{\beta}{s}+\eta, \quad (7)$$

and

$$\beta_s=(\phi-\eta)s,$$

where $D=[kT/(4\pi e^2n_e(\infty))]^{1/2}$, β_S is the normalized perturbing potential which satisfies a Poisson's equation in which only the free-electron density appears [13], $n_e(\infty)$

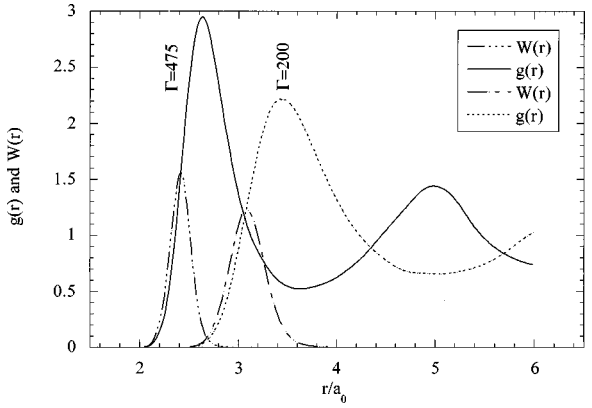

FIG. 1. Radial distribution functions $g(x)$ and the first neighboring ions $W(x)$ for $T=1$ eV for $\Gamma=200$ and 475.

$=[2(2\pi mkT)^{3/2}/h^3][2F_{1/2}(-\eta)/\pi^{1/2}]$ is the free-electron density [11], and the ratio $c^2/D^2=F_{1/2}(-\eta)$. Then Eq. (5) can be rewritten as

$$\Delta E_1(\rho,T)=-\frac{kT}{Z^*+1}\int_0^\infty [F_{1/2}(\beta/s,\beta/s+\eta) - F_{1/2}(\beta/s)g(s)]s\,ds. \tag{8}$$

Finally, the degeneracy term $\Delta E_{\rm deg}(\rho,T)$ represents the partial degeneracy of the free-electron state close to the ionization energy [17]. This term is computed by

$$\Delta E_{\rm deg}(\rho,T)=-\left(\frac{\beta_0}{b}\right)kT, \tag{9}$$

where β_0 is the value of β at the boundary $s=b$ ($a=cb$ is the atomic radius). Then the K-edge energy $E_1(\rho,T)$ can be given by Eq. (1) for various ionization stages.

The shape of the K edge can be found by averaging the absorption spectrum of the first shell ions around the central ion. In order to do this we must first find the first neighbor distribution function $W(r)$. This can be found from the radial distribution function $g(r)$ which, in turn, is found from the OCP model.

The OCP model is characterized by the Coulomb coupling parameter $\Gamma=(Z^*e)^2/akT$. From the TF model, the average ionization state Z^* can be calculated for a given density and temperature; then the value of Γ can be calculated. The radial distribution function $g(x)$ for values of Γ from 0.05 up to 160 were obtained from the tabulated Monte Carlo OCP values given in Refs. [7] and [8]. For values of Γ above 160, the values of $g(x)$ were obtained from hypernetted chain solutions to the OCP model given in Ref. [9].

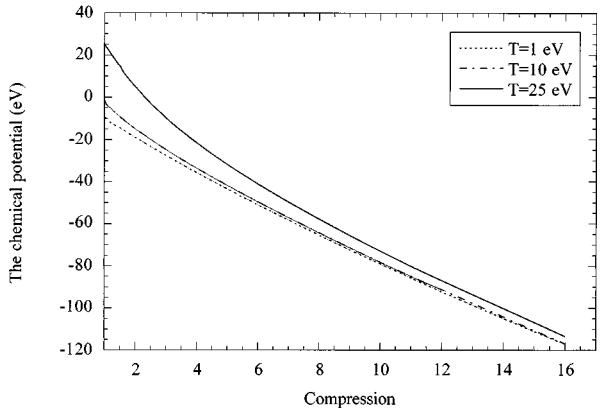

FIG. 3. Degeneracy term as a function of compression for $T=1$, 10, and 25 eV.

The absorption spectrum is given by

$$\mu(a,T)=n(a,T)\sigma(E_x,a), \tag{10}$$

where $\mu(a,T)$ is the absorption coefficient, $n(a,T)$ is the overall ion density, and $\sigma(E_x,a)$ is the absorption cross section for a single ion; and

$$n(a,T)=\rho W(r), \tag{11}$$

where $W(r)$ is the nearest neighbor distribution function. The distribution of neighboring ions $P(r)$ can be written as

$$P(r)dr=4\pi\rho g(r)r^2dr. \tag{12}$$

Then the first neighbor distribution is given by Mihalas [18] as

$$W(r)dr=P(r)dr\left[1-\int_0^r W(z)dz\right]. \tag{13}$$

By differentiation and resubstitution, we find

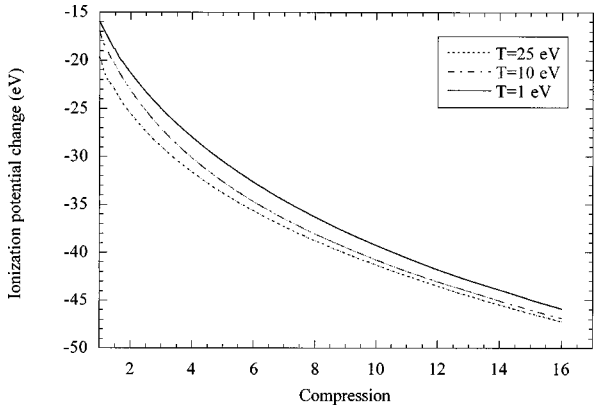

FIG. 2. Continuum lowering energy as a function of compression for $T=1$, 10, and 25 eV.

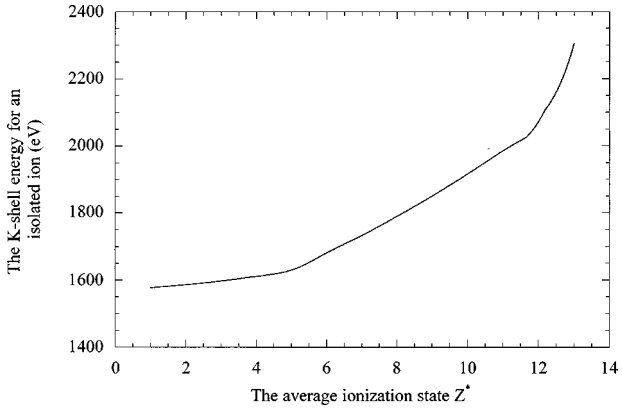

FIG. 4. K-shell ionization energy of an isolated ion as a function of the average ionization state.

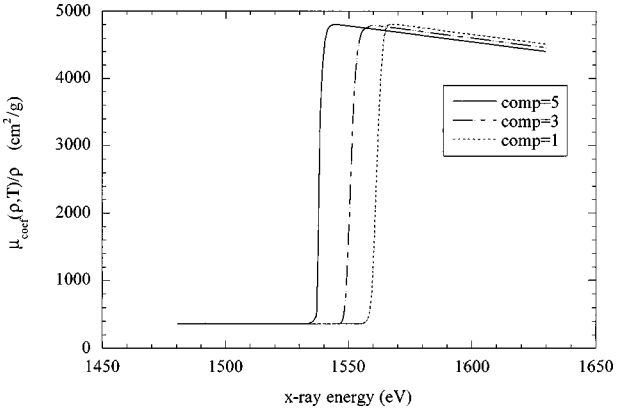

FIG. 5. Shows the absorption spectrum of the K edge for $T=1$ eV and compressions of 1, 3, and 5.

$$W(r)=C\left\{4\pi\rho g(r)r^2\exp\left[-4\pi\rho\int_0^r g(r)r^2dr\right]\right\}=C\overline{W}(r), \tag{14}$$

where the constant C is given by

$$\int_0^\infty W(r)dr=C\int_0^\infty \overline{W}(r)dr=1. \tag{15}$$

The single ion absorption cross section $\sigma(E_x,a)$ can be defined by

$$\sigma(E_x,a)=\sigma_0+q(E_x,E_1(\rho,T))\Delta\sigma, \tag{16}$$

where σ_0 is the initial value of the cross section, and $q(E_x,E_1(,T))$ is the correction factor to the K edge for the degeneracy [19], which is equal to

$$q(E_x,E_k(\rho,T))=\frac{1}{\left[1+\exp\left(\dfrac{E_x-E_1(\rho,T)}{kT}\right)\right]}, \tag{17}$$

where E_x is the x-ray energy.

Then Eq. (10) can be written as

$$\mu(a,T)=\rho W(r)\sigma_0+[\rho W(r)q(E_x,E_1(\rho,T))\Delta\sigma]. \tag{18}$$

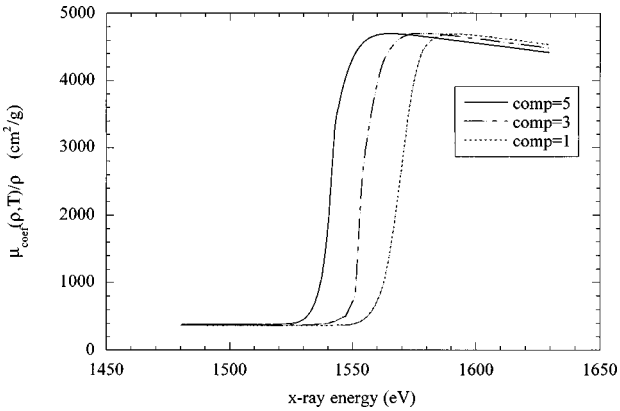

FIG. 6. Absorption spectrum of the K edge for $T=5$ eV and compressions of 1, 3, and 5.

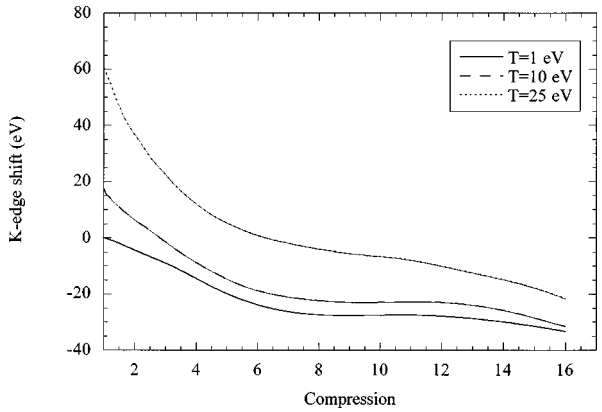

FIG. 7. Shift of the K edge as a function of compression for $T=1$, 10, and 25 eV.

The real value of the absorption coefficient is given by integrating the term $\mu(a,T)$ over a range of distance $(r,r+dr)$ and weighted with $W(r)$ as follows:

$$\mu_{\text{coef}}(a,T)=\frac{\int_0^r \mu(a,T)d^3r}{\int_0^r W(r)d^3r}. \tag{19}$$

Thus the shape and width of the K edge can be calculated for a given temperature and density.

III. RESULTS AND DISCUSSION

For any given radial distribution function $g(x)$, we can find a unique function for the first neighboring ions $W(x)$. Figure 1 shows an example of the variation of $g(x)$ and $W(x)$ as a function of the normalized x for a given value of Γ. This can be used for the calculation of the width of the K edge.

Results of our calculations of the continuum lowering term $\Delta E_1(\rho,T)$, the degeneracy term $\Delta E_{\text{deg}}(\rho,T)$, and the K-shell ionization energy of an isolated ions of aluminum as a function of the average ionization state $E_0(Z^*)$ are shown in Figs. 2, 3, and 4. These figures show that for the range of density and temperature considered, the continuum lowering contribution varies only slightly with temperature but varies strongly with density, whereas the degeneracy contribution increases with density but shows more dependence on tem-

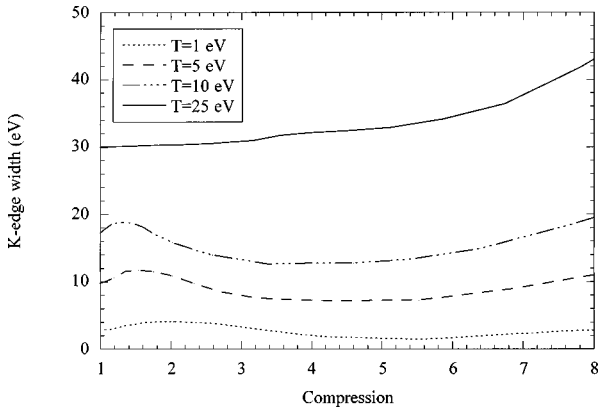

FIG. 8. Width of the K edge as a function of compression for $T=1$, 5, 10, and 25 eV.

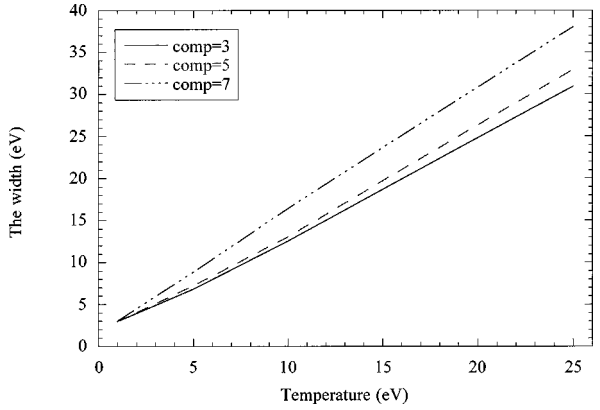

FIG. 9. Width of the K edge as a function of temperature for compressions of 3, 5, and 7.

perature. The increase in both $\Delta E_1(\rho,T)$ and $\Delta E_{\mathrm{deg}}(\rho,T)$ with temperature can be attributed to the increase in the average ionization state Z^*, which can lead to dramatic increase in the K-shell energy. The increase of $\Delta E_1(\rho,T)$ and $\Delta E_{\mathrm{deg}}(\rho,T)$ with temperature can also be attributed to the increase of the shift as we follow Eq. (1).

The calculated absorption spectrum of the aluminum K edge for $T=1$ and 5 eV, and for compressions of 1, 3, and 5, is presented in Figs. 5 and 6. These two figures show the changes in the shift and the width of the K edge with the temperature and the compression.

Figure 7 shows the shift of the K edge versus compression for these values of temperature. The K edge is shifted to the blue at high temperature and low compressions, and tends to shift toward the red as the compression increases and the temperature decreases. This happens due to the shift of the chemical potential from positive at low compression to negative at higher compression. The increase of the temperature leads to an increase in the value of the average ionization state, which, in turn, results in a higher value of K-edge energy for an isolated aluminum ion.

The effect of the temperature on the width of the K edge is larger than the effect of the compression. The increase of the temperature produces a wider peak of the first neighboring ions, and that leads to a larger value of the width. Figures 8 and 9 show that the width of the K edge is strongly temperature dependent rather than compression dependent.

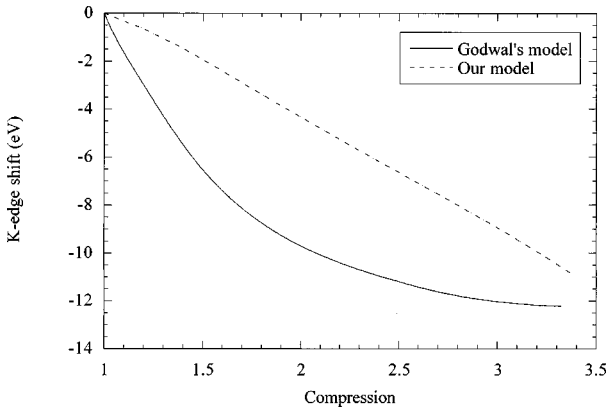

FIG. 10. Comparison between our model and the Godwal and Lee model [2] for the K-edge shift vs compression.

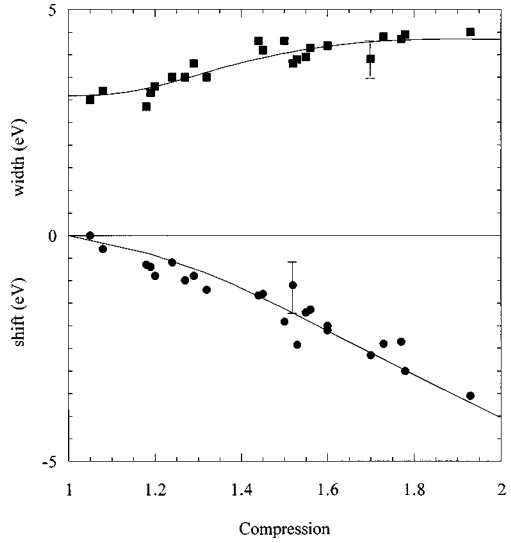

FIG. 11. Comparison of the experimental results (● and ■) and the results of the model (continuous lines) plotted against compression.

Figure 10 shows a comparison of the K-edge shift between this model and Godwal's and Lee's model [2] over a range of compression ratios from 1 to 3.3 and a temperature of 1 eV. The shift predicted by our model is approximately half that predicted by the model of Godwal and Lee over the range of their results.

The model has been used to predict the shift and width of the absorption edge in experiments carried out by Hall *et al.* in Paris [20]. In this experiment, a thin aluminum layer is sandwiched between two plastic tamper layers. The aluminum is compressed by laser driven shock waves driven from either side in the plastic layers, so the shock waves collide in the aluminum. A synchronized short pulse laser is incident on a uranium target to produce a continuum x-ray backlighter source around the K-absorption edge of the aluminum. The absorption spectrum is obtained using a thallium acid phthalate (TlAP) flat crystal spectrometer and recorded on an x-ray charge coupled detector (CCD) camera (full details of the experiment are given in Ref. [20]). The compression and temperature at the time of measurement can be changed by varying either the laser shock drive energies or the relative timing of the shock drive and backlighter pulses. Results for the shift and the width for both the model and the experiment are shown in Fig. 11. The experiment was only able to achieve maximum compressions $\approx\times 2$ and temperatures of ≈ 1 eV, but within this range the agreement between experiment and model for both the shift and the width is excellent.

IV. CONCLUSIONS

By determining the absorption spectrum of individual ions and using a local ion distribution function, we have been able to show that it is possible to predict both the shift and shape of the absorption edge of aluminum, unlike previous models which have only been able to predict the shift. It is shown that by measuring both the shift and width of the absorption edge, an independent measurement of the density and temperature of the plasma can be made. The shift of the edge predicted by this model has been compared with exist-

ing models such as Godwal and Lee [2] under similar circumstances, and, while the same general form of the shift is found, in our case the shift is about half of that predicted in Ref. [2]. However, the strength of our model lies particularly in its ability to predict the shape and position of the absorption edge over a large range of compressions and temperature.

ACKNOWLEDGMENTS

The authors would like to thank A. Djaoui and S. Rose for providing the Hartree-Fock *K*-shell energies. This work was supported by EU Human Capital and Mobility project ''Dense Plasmas and Laser Compression,'' under Contract No. CHRX-CT93-0338.

[1] D. K. Bradley, J. Kilkenny, S. J. Rose, and J. D. Hares, Phys. Rev. Lett. **59**, 2995 (1987).
[2] B. K. Godwal and Y. T. Lee, Phys. Rev. A **40**, 8 (1989).
[3] L. Da Silva, A. Ng, B. K. Godwal, G. Chiu, F. Cottet, M. C. Richardson, P. A. Jaanimagi, and Y. T. Lee, Phys. Rev. Lett. **62**, 1623 (1989).
[4] H. Motz, *The Physics of Laser Fusion* (Academic, New York, 1967).
[5] H.-D. Frey and J. Meyer-ter-Vehn, Contrib. Plasma Phys. **37**, 77 (1997).
[6] H.-D. Frey and J. Meyer-ter-Vehn, Contrib. Plasma Phys. **37**, 89 (1997).
[7] S. G. Brush, H. L. Sahlin, and E. Teller, J. Chem. Phys. **45**, 2102 (1966).
[8] W. L. Slattery, G. D. Doolen, and H. E. Dewitt, Phys. Rev. A **21**, 2087 (1980).
[9] Kin-Chue Ng, J. Chem. Phys. **61**, 2680 (1974).
[10] B. F. Rozsnyai, Phys. Rev. A **5**, 1137 (1972).
[11] J. C. Stewart and K. D. Pyatt, Astrophys. J. **144**, 1203 (1966).
[12] H. A. Bethe and R. M. Jackiw, *Intermediate Quantum Mechanics*, 3rd ed. (Benjamin/Cummings, Menlo Park, CA, 1968), p. 83.
[13] R. P. Feynman, N. Metropolis, and E. Teller, Phys. Rev. **75**, 1561 (1949).
[14] R. M. More, Adv. At. Mol. Phys. **21**, 305 (1985).
[15] A. K. McMahan and M. Ross, *High Pressure Physics in Science and Technology* (Gordon and Breach, New York, 1968), Vol. 7.
[16] B. K. Godwal, Phys. Rev. A **28**, 1103 (1983).
[17] J. P. Cox, *Principles of Stellar Structure* (Gordon and Breach, New York, 1968), Vol. 1.
[18] D. Mihalas, *Stellar Astrophysics*, 2nd ed. (Freeman, San Francisco, 1978).
[19] S. J. Rose, *Laser Plasma Interaction*, Proceedings of the Thirty-Fifth Scottish Universities Summer School in Physics (The Scottish Universities Summer School in Physics, Edinburgh, 1988).
[20] T. A. Hall, J. Al-Kuzee, A. Benuzzi, M. Koenig, J. Krishnan, N. Grandjouan, D. Batani, S. Bossi, and S. Nicollela, Europhys. Lett. **41**, 495 (1998).